Current Science
CS 5 (5), 4903-4917 (2025)
Received 28 July 2025 | **Revised 18 August** 2025 | **Accepted 08 September** 2025 | **Online Available 18 October** 2025
https://doi.org0/10.52845/CS/2025-5-5-43

Current Science

Current Science

OPEN ACCESS

ISSN(O) 2795-8639

Original Article

A Case of Primary Intracranial Angiomyoma and Review of the Literature

Aixin Ou[¶], Xiangxuan Zhao[#§*]

[#]College of Laboratory Animal Medicine, Liaoning University of Traditional Chinese Medicine, Shenyang 110847, China

[§]College of Pharmacy, Liaoning University of Traditional Chinese Medicine, Dalian 116600, China.

[¶]Department of Radiology, Shengjing Hospital of China Medical University, Shenyang 110004, LN, China

[*]Corresponding Author: Xiangxuan Zhao

Abstract:

Background. A rare presentation of angiomyoma (also called angioleiomyoma or ALM) is primary intracranial ALM (ICALM). This benign tumor is more common in men aged 40-60 years but its etiology remains unclear. Because of limited reports, atypical clinical manifestations and imaging features, ICALM is often misdiagnosed.

Methods. We describe the case of a 58-year-old male ICALM patient admitted with intermittent left side headaches and conduct a literature review to summarize the key clinical, imaging and pathological features of all known cases of ICALM.

Results. Only 53 known cases of ICALM have been previously reported and we describe the first case instance located in the left cerebellopontine angle area. This patient's preoperative magnetic resonance imaging (MRI) imaging showed homogeneously T1-weighted low signal, slightly T2-weighted high signal and the diffusion weighted imaging (DWI) slightly low signal, which was consistent with the MRI features of known cases of ICALM. The patient underwent tumor resection through the right retrosigmoid sinus approach with an uneventful postoperative course and no long-term complications. Pathological diagnosis confirmed ICALM with tumor cells positive for smooth muscle actin and negative for neurological, mesenchymal and epithelial markers. Analysis of the literature showed that the cavernous type of ICALM was most common with our case example being a mixture of solid and cavernous types.

Conclusions. The progressive enhancement of MRI can contribute to ICALM diagnosis with pathological confirmation by immunohistochemistry. The first-line treatment strategy for ICALM is surgical resection, which can lead to good outcomes.

Key words: intracranial angiomyoma ; diagnosis ; prognosis ; MRI ; CT

Introduction

ALM is a benign tumor recognized as an independent tumor entity by the World Health Organization (WHO) in 2016 mostly found in women [1]. It is usually considered as a benign tumor that mostly occurs in the dermis and subcutaneous tissue of the lower limbs of middle-aged and elderly individuals where it mainly manifests as subcutaneous nodules [2]. Compared with ALM, primary intracranial ALM (ICALM) is relatively rare. Due to its atypical clinical and imaging features, ICALM is often misdiagnosed and may be confused with other diseases including meningiomas and schwannomas.

To date, the cause of ICALM is still unclear. Some studies have suggested that ICALM may be

related to Epstein-Barr virus (EBV) infection and results from the effects of induced immune suppression [3]. However, this notion is not universally supported by other researchers [4]. Nonetheless, because of the scarcity of ICALM and limited clinical information available, a relationship between ICALM and EBV infection and/or immunosuppressive diseases cannot be completely ruled.

Herein, we reported a case of ICALM, described its clinical, imaging and pathological features, and conducted an analysis of all 53 known cases of ICALM reported in the literature.

Methods

Details of Case Report

The study was conducted with the approval of The Research Ethics Committee of Shengjing Hospital of China Medical University with informed consent provided by the patient. The patient was treated in the first Department of Neurosurgery, Shengjing Hospital of China Medical University on April 23, 2018. Imaging and pathological data were provided by the Department of imaging and pathology, respectively, Shengjing Hospital of China Medical University. Signa HDxT (3.0T) was used for MRI imaging and Siemens Somatom Definition and Philips iCT 256 used for the CT scans. The Roche Ventana automated immunohistochemical (IHC) system was used for IHC analysis with the primary antibodies used as follows: rabbit anti-human CD34 antibodies (clone EP88, ZSGB-BIO); mouse anti-human smooth muscle actin (SMA) antibodies (clone UMAB237, ZSGB-BIO); rabbit anti-human S-100 anti-bodies (ZSGB-BIO); rabbit anti-human Vimentin antibodies (clone EP21, ZSGB-BIO); rabbit anti-human glial fibrillary acidic protein (GFAP) antibodies (clone EP13, ZSGB-BIO); rabbit anti-human Desmin antibodies (clone EP15, ZSGB-BIO); mouse anti-human epithelial membrane antigen (EMA) antibodies (clone UMAB57, ZSGB-BIO); rabbit anti-human progesterone receptor (PR) antibodies (Roche); and rabbit anti-human monoclonal Ki-67 (MIB-1) antibodies (clone 30-9, Roche).

Literature Search

The retrieval query ("angioleiomyoma" OR "vascular leiomyoma" OR "angiomyoma" OR "ALM") AND ("intracranial " OR "brain" OR "cranial" OR "head" OR "CNS") was used to collect reports in the Pubmed and CNKI databases. Extracranial angiomyoma cases were excluded.

Results and Discussion

Case Report

Patient History and Diagnostic Imaging

A 58-year-old male patient was admitted to the hospital with intermittent headaches as the main complaint. The patient reported the symptoms first occurred three years before, with recurring headaches on the left side with no obvious cause, no dizziness, and tolerable pain levels. No prior systematic diagnosis or treatment was given to the patient before hospital admission. Nervous system examination showed that the left ear had decreased hearing or hearing loss, but there were no apparent abnormalities present for other sense organs.

Preoperative MRI imaging showed homogeneously T1-weighted low signal and slightly T2-weighted high signal **(Figure 1A-B),** and DWI signal was slightly low **(Figure 1C)**, demonstrating that the tumor contour in the left cerebellopontine angle area was clear. Noncontrast head CT showed a slightly hyperdense mass (about 2.8 cm×1.7 cm) with no internal calcification and no surrounding edema in the left cerebellopontine angle area with no obvious enhancement **(Figure 1D-E)**. The adjacent cerebellar hemisphere was compressed. An initial diagnosis of meningioma was made.

Surgery and Postoperative Course

The patient underwent tumor resection through the left retrosigmoid sinus approach. After incision of the dura, the tumor was found to have a complete capsule, which originated from the dura of the posterior fossa. Cranial nerves VII-VIII were compressed. After incision of the tumor capsule, the tumor was of solid and tough consistency with a limited blood supply. After tumor decompression, the tumor capsule adhering to the brainstem and cerebellar hemisphere was stripped and the tumor then removed. Artificial dura mater was used to repair the defect of the dura mater, and a skull repair plate used. Intraoperative blood loss during the surgical process was approximately 10 mL. Noncontrast head CT confirmed complete resection of the lesion **(Figure 1F)**. No adverse events occurred during the patient's postoperative course and after resection, the patient's headaches disappeared and hearing somewhat recovered. Follow-up conducted by telephone interview indicated no sign of recurrence after 31 months.

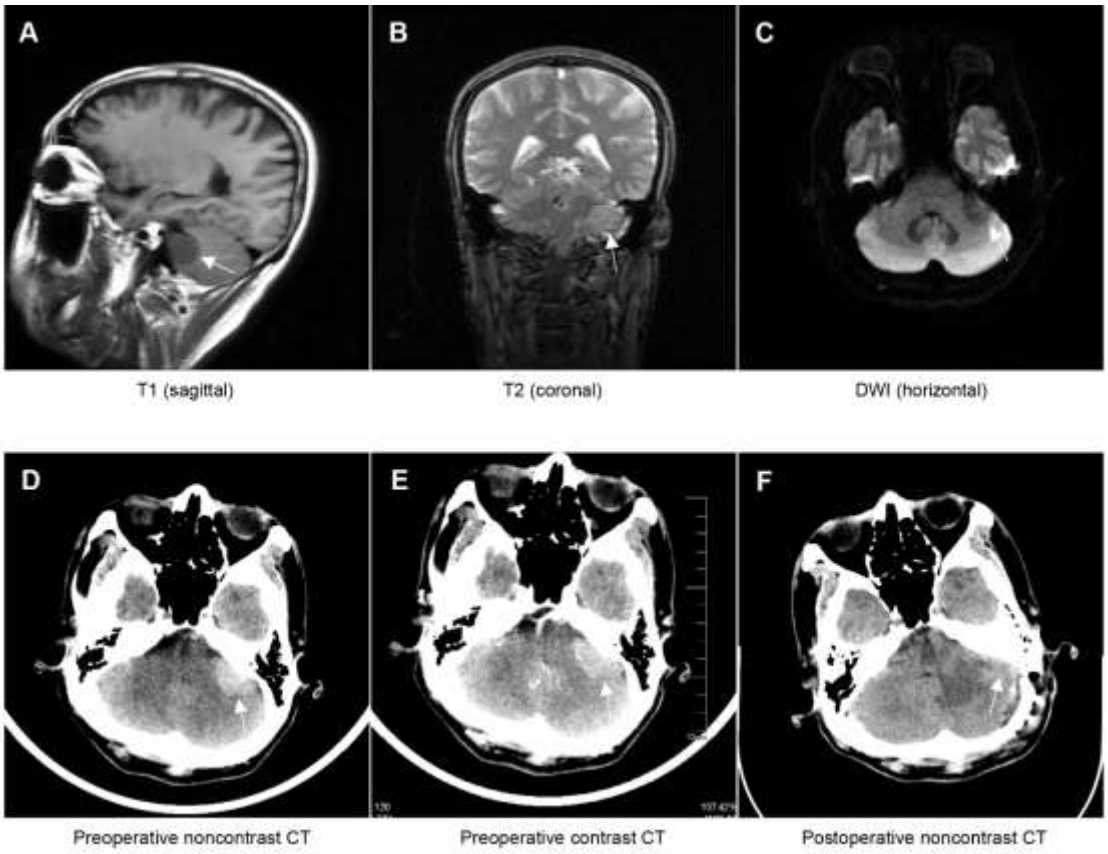

Figure 1. Image data of patients before and after surgery.

A: MRI T1-weighted sequence showed a homogeneously low signal at the left cerebellopontine angle in the sagittal positions. **B**: MRI T2-weighted sequence showed a slightly high signal at the left cerebellopontine angle in the coronal positions. **C**: DWI sequence showed a slightly low signal at the left cerebellopontine angle in the horizontal positions. **D-E**: Noncontrast CT scan showed that the tumor in the left cerebellopontine angle area with slightly hyperdense, no calcification and edema. The contrast scan showed no obvious enhancement. **F**: Postoperative CT scan showed complete tumor resection.

Histopathology

The lesion displayed irregular vascular cavities with different sizes and shapes. Examination of H&E sections showed that the tumor was composed of large numbers of blood vessels and

spindle cells with interstitial fiber hyperplasia **(Figure 2A)**. The spindle cells were closely connected, crossed each other, and were located around the blood vessels. No nuclear atypia, mitotic activity, and signs of necrosis were found in the tumor. Immunohistochemistry results showed that vascular endothelial cells were positive for CD34 **(Figure 2B).** SMA was expressed in the perivascular spindle cells, whereas Vimentin, Desmin, EMA, GFAP, PR, and S-100 staining were negative (**Figures 2C-H)**. The Ki-67 positive index in tumor cells was less than 1%. The pathological diagnosis was ICALM in the left cerebellopontine angle.

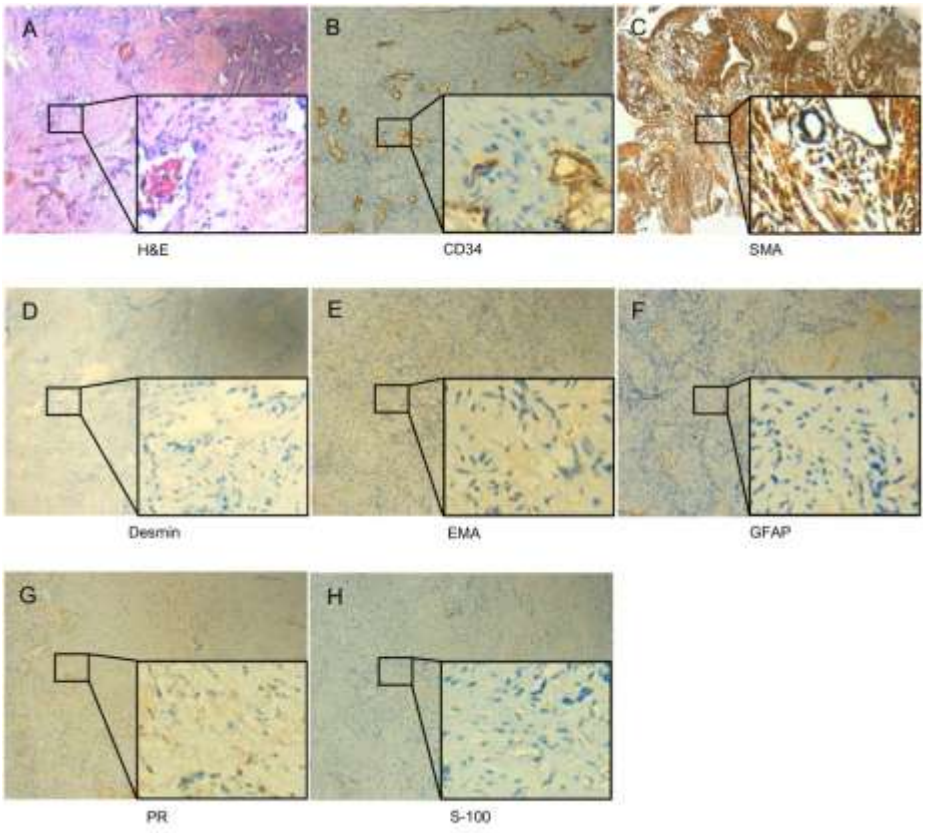

Figure 2. Histopathology and immunohistochemistry analysis of ICALM.

A: H&E staining showed that the tumor was composed of a large number of blood vessels and spindle cells. The spindle cells were closely connected, cross each other, and are located around the blood vessels (magnification: 50×). **B**: Immunohistochemistry showed that tumor vascular endothelial cells were positive for CD34 (magnification: 100×). **C-D**: Immunohistochemistry showed that spindle cells were positive for SMA and negative for DEM (magnification: 50×). **E-H**: Immunohistochemistry showed negative staining for EMA, GFAP, PR, and S-100 (magnification: 100×).

Literature Review Findings

Since the first reported case of primary ICALM demonstrated by Lach et al. in 1994[5], our literature review identified a total of 53 cases reported to date. Together with our new case and those obtained from our literature search we then analyzed the clinical, imaging, and pathological characteristics of all 54 reported incidences of ICALM.

Clinical Features of ICALM

The summary of the available clinical data for the 54 known cases of ICALM is shown in **Table 1**. ICALM was more common among men (male: female 33:20) which contrasts the profile of ALM which is most prevalent in women [1]. ICALM patients have reported over the age range from 5

to 77 years old but was more common in middle-aged people 40-60 years (32/54, 59.26%). The clinical manifestations of ICALM were non-specific and inconsistent. The main symptomatic manifestations were consistent with local intracranial compression, of which intracranial hypertension and headache being the most common (22/54, 40.74%).

Previous reports indicate that ICALM is often located closely to the venous sinus and cranial plate block and may invade the dura mater [5, 6]. Our analysis indicated the most frequent presentation was in the cavernous sinus (14/54, 25.93%). In addition, we identified two cases of invasion of the frontal bone (2/54, 3.70%). Although ICALM is mostly a single-center lesion, there are some reports showing exceptions, for example, Ravikumar *et al.* reported that patients with ICALM had two lesions located at the head of the caudate nucleus on the right and the globus pallidus on the left [7]. Shinde *et al.* reported a case of primary multiple ICALM [8], which invaded the putamen, hippocampus, optic nerve and pia mater. To our knowledge, our report is the first case showing ICALM located in the left cerebellopontine angle area.

Table 1. Clinical data summary of primary ICALM

Study	Sex/Age (years)	Clinical symptoms	Location	Size(cm)	Therapy	Rec	Follow-up (months)
Lach et al.1994[5]	M/47	RT sided limp; RT hand incoordination	RT parietal lobe	2.7×2.0×2.0	GTR	NR	48
Ravikumar etal.1996[7]	F/12	Diffuse dull aching headache; occasional diplopia of two months	Basal ganglionic	5.0	GTR	NR	20
Kohan et al.1997[20]	NA/NA	Hearing loss; tinnitus	IAM	NA	GTR	NA	NA
Figueiredo et al.2005[18]	M/52	Headache; diplopia; visual deficit; facial numbness	RTCS	6.0×6.0×5.0	GTR	NA	NA
Karagama et al.2005[24]	F/47	Hearing loss in the LT ear; occasional vertigo	IAM	NA	GTR	NR	12
Colat-Coulbois et al.2008[9]	M/50	Acute transient headache; diplopia	LTCS	NA	GTR	NR	72
Vijayasaradhi et al. 2008[25]	F/10	Small swelling on the LT forehead region	LT frontal bone	4.0×3.0	GTR	NA	NA
Liu et al.2009[11]	M/50	Frontal headache for 6 months; occasional seizures attacks	Cerebral falx	4.0×4.0×3.0	GTR	NR	18
Gasco et al.2009[4]	M/43	Acute-onset headache; blurred vision; dizziness; gait abnormalities	LT cerebellar hemisphere	4.4 × 3.9 × 3.9	GTR	NR	NA
Xu et al.2010[3]	M/53	Headache for 3 months	Sellar region	<1	GTR	NR	6
Pepper et al.2010[26]	F/13	Hearing loss and headache	IAM	NA	GTR	NA	NA

Conner et al.2012[27]	M/42	Poorly localized headache for 8 years	Superior RT cerebellar hemisphere	0.8-1	GTR	NA	23
	M/36	Worsening daily headache	Cerebral falx, corpus callosum	2.5	STR	NR	26
Shinde et al.2012[8]	M/60	Progressive headache for two months; seizures; irritability	RT: putamen; LT: hippocampus	RT: 2; LT: NA	Autopsy	Died	
Zhou et al.2012[28]	M/62	Seizures	Middle cranial fossa	3.7×3.5×3.3	GTR	NA	14
Lescher et al.2014[17]	M/40	Headaches; epilepsy with tremor of the LT half of the body	Cerebral falx	NA	GTR	NA	NA
Da et al.2014[21]	F/23	Impaired RT visual acuity for 8 years	LTCS	5.5×5.5×5.7	STR	NR	6
	M/62	Hypophrasia, and mild disturbance of consciousness for 2 months	RT temporal lobe	2.5×3.5×3.5	GTR	NA	NA
Sun et al.2014[6]	F/51	Long blurry of the RT eye for 2 months	Sella region	3.0×2.5×2.5	GTR	Died#	
Sun et al.2014[6]	M/49	Weakness in the lower limbs; sporadic falling down; dizziness	Tentorium cerebelli	4.2×4.6×5.7	STR	NR	12
Sun et al.2014[6]	M/77	Intermittent headache for five months	LT temporal lobe	1.6×3.1×3.9	GTR	NR	12
Teranishi et al.2014[32]	F/52	RT eye discomfort for 6 months	RTCS	2.3	GTR	NR	0.5
He et al.2014[30]	F/46	Headache for 1 year; blepharoptosis in the RT eye for 4 months	CS	2	GTR	NR	72
	M/57	Headache for 10 years; vision loss and diplopia for 3 months.	CS	3	GTR	NR	57
	F/48	Headache for 7 years; RT severe ptosis for 1 year	CS	3	GTR	NR	47
	F/35	Headache for 1 year; decreased LT vision and diplopia for 1 week	CS	2	GTR	NR	14
Lin et	M/36	Worsening daily	RTCS	5.0×6.0	STR*	NR	20

al.2015[19]		headache and diplopia for 2 months		×6.0			
Calle et al.2016[31]	M/43	Light-headed for 5-10 minutes	Anterior flax cerebri	1.6	GTR	NR	NO
Li et al.2016[22]	M/64	LT eye blurred for 6 months	Sellar region	NA	Biopsy + γknife	Shink &	48
	F/40	Vision decreased; diplopia; menstruation and lactation stopped	Sellar region	NA	PR+ γknife	NA	Lost visit
Delgado-Fernandez et al.2016[32]	M/43	Hearing loss	Infratentorial	1.4	GTR	NR	24
	M/19	Accidental	NA	NA	GTR	NR	12-120
Li et al.2018[10]	M/42	Vertigo; tinnitus; headache	RT CPA	2.0×2.2×2.3	GTR	NR	37.3
	M/43	Accidental	RT tentorium	2.9×2.7×2.7	GTR	NR	29
	M/58	Accidental	RT parietal lobe	2.6	GTR	NR	47.3
	M/48	Diplopia	RTCS	2.9×2.6×2.6	GTR	NR	46.4
	M/41	RT cranial nerve, VI pals	RTCS	2.1×1.7×1.9	GTR	NR	8.3
	F/47	LT visual deficit	LTCS, optic cannal	3.1	GTR	NR	33.9
	M/58	LT visual deficit	LT sellar	1.0	STR	NR	7.9
	M/53	Accidental	Bilateral cerebral falx	3.0	GTR	NR	5
Altieri et al.2019[13]	M/37	Accidental	LT tentorial posterior cranial fossa	3.9	GTR	NR	NA
Selbi et al.2019[33]	F/60	A complete RT sixth nerve palsy, diplopia	RT middle cranial fossa	NA	STR+ γknife	NR	48
Lee et al.2019[12]	F/56	Eyeball pain and blurred vision on her RT side for 4 years	RT orbital apex	NA	GTR	NA	NA
Chen et al.2020[34]	F/59	Epileptic seizures, progressive headache for 2 months	RT CS	1.3×1.1×1.1	GTR	NA	NA
Ding et al.2020[14]	F/35	LT leg claudication for one year	Lateral ventricles	6.3×7.4×5.4	GTR	NR	5
Zhang et al.2020[35]	M/15	RT nose obstruction,	RT frontal cranial base	3×2.5×2.5	GTR	NA	NA

		rhinorrhea, frontal headache for 2 years					
Current case	M/58	Intermittent LT headache for 3 years	LT CPA	2.8×1.7	GTR	NR	31
Abbreviations: CPA: Cerebellopontine angle; CS: cavernous sinus; F: female; GTR: gross total resection; IAM: internal acoustic meatus; LT: left; M: male; NA: not available; NR: no recurrence; STR: subtotal resection;*: STR three months later: Cyber knife treatment; #: Died of massive epistaxis 13 days after operation; Rec: recurrence; RT: right; &: The tumor continued to shrink;							

Imaging features of ICALM

CT scan results showed that most ICALM lesions were high density (18/23, 78.26%) (**Table 2**). Reports of MRI imaging further demonstrate that 70% of the cases showed T1-weighted low signal and T2-weighted high signal (28/40, 70.00%). After gadolinium injection, most showed nonhomogeneous enhancement (29/40, 72.50%) with a special form of enhancement: progressive enhancement (16/40, 40.00%), i.e., the images were "flame-like". The early stage of enhancement shows patchy enhancement in the center of the lesion, while the later stage gradually enhances from the center to the periphery. Starting from the center of the lesion, the enhancement spreads to the periphery of the tumor in a time-dependent manner [9]. This enhancement mode may be related to the tumor vascular structure [6, 10]. These enhancement features may be characteristic manifestation of ICALM and may help its early and/or differential diagnosis. Gadolinium injection CT scanning our case showed no enhancement which further confirmed the characteristics of the tumor's denseness and limited blood supply.

Table 2. Imaging features summary of primary ICALM

Study	CT			MRI				
	Density	**Edema**	**En**	**T1**	**T2**	**DWI**	**En**	**PE**
Lach et al.1994[5]	Hypo	Little	Hen	NA	NA	NA	NA	NA
Ravikumar et al.1996[7]	RT: Hypo LT: Hyper	None NA	nHen Hen	NA NA	NA NA	NA NA	NA NA	NA NA
Kohan et al.1997[20]	NA	NA	NA	NA	NA	NA	NA	NA
Figueiredo et al.2005[18]	Hyper	None	Hen	Iso	Hyper	NA	Hen	PE
Karagama et al.2005[24]	NA	NA	NA	NA	NA	NA	NA	NA
Colat-Coulbois et al.2008[9]	NA	NA	NA	Hypo	Hyper	NA	nHen	PE
Vijayasaradhi et al. 2008[25]	Hypo	None	None	NA	NA	NA	NA	NA
Liu et al.2009[11]	Mild hyper	None	Hen	Hypo	Hyper	NA	Hen, dural “tail sign”	NA
Gasco et al.2009[4]	Hyper	None	NA	Iso	Hyper	NA	Hen	NA
Xu et al.2010[3]	NA	NA	NA	Hypo	Hyper	NA	NA	NA
Pepper et al.2010[26]	NA	NA	NA	Iso	Iso	NA	Hen	NA
Conner et al.2012[27]	NA	NA	NA	NA	Hyper	None	nHen	NA
	Hyper	None	Hen	NA	NA	NA	NA	NA

Shinde et al.2012[8]	NA	NA	NA	Hypo	Hyper	NA	Hen	NA
Zhou et al.2012[30]	NA	NA	NA	Hypo	Hyper	Hypo	nHen, dural "tail sign"	NA
Lescher et al.2014[17]	NA	NA	NA	Iso	Hyper	Hyper	Hen	NA
*Da et al.2014[21]	Hyper	None	NA	Hypo	NA	NA	nHen	NA
	Hyper	Severe	NA	Iso	NA	NA	Hen, dural "tail sign"	NA
Sun et al.2014[6]	NA	NA	NA	Iso	Hyper	NA	nHen	PE
Sun et al.2014[6]	NA	NA	NA	Hypo	Hyper	NA	nHen	PE
Sun et al.2014[6]	NA	NA	NA	Iso	Hyper	NA	Hen	NA
Teranishi et al.2014[29]	Hyper	None	nHen	Iso	Hyper	NA	nHen	PE
He et al.2014[30]	Hyper	None	NA	Hypo	Hyper	NA	nHen	PE
Lin et al.2015[19]	Mild hyper	None	NA	Hypo	Hyper	NA	nHen	NA
Calle et al.2016[34]	Hyper	None	NA	Iso	Hyper	NA	Hen	PE
Li et al.2016[22]	Mild hyper	None	NA	Hypo	Hyper	NA	nHen	NA
	Mild hyper	None	NA	Hypo	Hyper	NA	nHen	NA
Delgado-Fernandez et al.2016[32]	Hyper	None	Hen	Iso	Hyper	NA	nHen	PE
Li et al.2018[10]	Hyper	None	NA	NA	NA	NA	NA	NA
	NA	NA	NA	Hypo	Hyper	NA	nHen	NA
	NA	NA	NA	Hypo	Hyper	NA	nHen	NA
	NA	NA	NA	Hypo	Hyper	NA	nHen	PE
	NA	NA	NA	Hypo	Hyper	NA	nHen	PE
	NA	NA	NA	Hypo	Hyper	NA	nHen	NA
	NA	NA	NA	Hypo	Hyper	NA	nHen	NA
	NA	NA	NA	Hypo	Hyper	NA	nHen	NA
Altieri et al.2019[13]	Mild hyper	None	NA	Hypo	Hyper	NA	nHen	PE
Selbi et al.2019[33]	NA	NA	NA	NA	NA	NA	nHen	NA
Lee et al.2019[12]	NA	NA	NA	Iso	Hyper	NA	Hen	NA
Chen et al.2020[34]	NA	NA	NA	Hypo	Hyper	NA	nHen	PE
Ding et al.2020[14]	NA	NA	NA	Hypo	Hyper	Hyper	nHen	PE
Zhang et al.2020[35]	Mild hyper	Severe	NA	Hypo	Hyper	NA	nHen	PE
Current case	Mild hyper	None	NA	Hypo	Hyper	Hypo	None	NA

Abbreviations: DWI: diffusion weighted imaging; En: enhancement; Hen: homogeneous enhancement; nHen: nonhomogeneous enhancement;Hyper: hyperdense; Iso: isodense or isointense; Hypo: hypodense or hypointense; MRI: magnetic resonance imaging; NA: not available; OC: Osteolytic changes; PE: progressive enhancement; T1: T1-weighted gradient echo; T2: T2-weighted gradient echo; *: There was calcification in CT examination

Pathological Characteristics of ICALM

ICALM lesions are mainly composed of well-differentiated smooth muscle cells and endothelial cells. Loose mature smooth muscle bundles are located around blood vessels or interspersed between blood vessels, forming many vascular channels containing varying amounts of collagen

[2]. According to the ratio of smooth muscle cells and endothelial cells, ICALM can be divided into three types: 'solid' which is mainly composed of dense smooth muscle cells (**Table 3**). While some scholars believe that ICALM is of venous origin.

Since small arteries and mature adipose tissue can be found in ICALM, some reports argue that these lesions are a form of hamartoma [5]. Cytogenetic changes have also been reported in ICALM [3] although there is currently insufficient data to indicate whether there are commonly encountered genetic changes. Consistent with our case study, most ICALM cells do not show nuclear atypia nor high mitotic activity. However, Sophie et al. reported that ICALM occasionally may also contain focal, mild nuclear atypia and regular albeit low mitotic characteristics [3].

Table 3. Pathological summary of primary ICALM

Study	Immunohistochemical characteristics		Pathology type
	(Positive)	(Negative)	
Lach et al.1994[5]	VIM, DES, SMA, Myosin, NSE, PCNA, MIB-1(4.22%)	GFAP, AE1, AE3, NF, S-100, Ulex- europaeus, Endothelin, FVIII-RAg	Venous
Ravikumar et al.1996[7]	DES	S-100, GFAP	Solid
Kohan et al.1997[20]	NA	NA	NA
Figueiredo et al.2005[18]	SMA, VIM, CD34	S-100, EMA, GFAP, MSA	Cavernous
Karagama et al.2005[24]	SMA	NA	Cavernous
Colat-Coulbois et al.2008[9]	CD31, SMA, VIM, CD34	EMA	Cavernous
Vijayasaradhi et al. 2008[25]	SMA	EMA, VIM, S-100	Solid
Liu et al.2009[11]	SMA, VIM	EMA, S-100, GFAP	NA
Gasco et al.2009[4]	SMA, CD34	EMA	Cavernous-venous
Xu et al.2010[3]	CD41, CD34, SMA, MSA, DES, VIM, EBV	Keratin, EMA, GFAP, S-100	Cavernous
Pepper et al.2010[26]	NA	NA	NA
Conner et al.2012[27]	SMA, MSA, VIM	DES, CD34, EMA, S-100	Cavernous
	SMA, MSA, VIM	DES, CD34, EMA, S-100	Cavernous
Shinde et al.2012[8]	SMA, VIM, DES	GFAP, EMA, CD31, CD34, MIB-1	NA
Zhou et al.2012[28]	SMA, DES, VIM, S-100	EMA, CK, GFAP, HMB-45, p53, p16	Venous
Lescher et al.2014[17]	CD34, SMA	NA	NA
Da et al.2014[21]	SMA, VIM, CD34, S-100, EMA	GFAP, SYN, Chromogranin A, CK, MIB-1	NA
	SMA, VIM, CD34, DES	D2-40, S-100, PR, EMA, HMB45, CK, MIB-1	Cavernous
Sun et al.2014[6]	VIM, SMA, CD34	GFAP, NF	NA
Sun et al.2014[6]	VIM, SMA, CD34	EMA, Inhibin-a	NA
Sun et al.2014[6]	VIM, SMA, CD34	NA	NA
Teranishi et al.2014[29]	CD34, SMA, Caldesmon, Alponin	EMA, S100	Cavernous
He et al.2014[30]	SMA, CD34, S100	MIB-1	Cavernous
Lin et al.2015[19]	VIM, SMA, CD31, CD34	EMA, S-100, PR	NA
Calle et al.2016[31]	SMA, CD31	NA	Solid
Delgado-Fernandez et al.2016[32]	SMA, Caldesmon	NA	Solid

Li et al.2018[10]	SMA, VIM, CD34, DES	EMA, PR	Cavernous
	SMA, VIM, CD34	DES	Cavernous
	SMA, VIM, CD34	DES, S-100, CK	Cavernous
	SMA, VIM, CD34	DES	Cavernous
	SMA, VIM, CD34	DES	Cavernous
	SMA, VIM, CD34	DES	Cavernous
	SMA, VIM, CD34	DES	Cavernous
	SMA, VIM, CD34	DES	Cavernous
Altieri et al.2019[13]	SMA, DES, Caldesmon, CD31	GFAP, CD34, STAT-6	NA
Selbi et al.2019[33]	SMA, CD34, S-100	DES	NA
Lee et al.2019[12]	SMA	NA	NA
Chen et al.2020[34]	CD31, CD34, D2-40, Caldesmon, SMA, SSTR2, DES, EMA	CD56, GFAP, PR, S-100, HMB-45	NA
Ding et al.2020[14]	SMA, Calponin, CD34	S-100, DES, SSTR2	NA
Zhang et al.2020[35]	VIM, DES, MSA, HHF-35, SMA, CD34	S-100, Myogenin, NSE	NA
Current case	CD34	S-100, VIM, PR, GFAP, EMA	NA

Abbreviations: CD31: Cell differentiation factor 31; CD34: Cell differentiation factor 34; DES: desmin; EBV: Epstein-Barr virus; EMA: epithelial membrane antigen; FVIII-RAg: Factor VIII-related Antigne; GFAP: glial fibrillary acidic protein; MSA: muscle specific actin; NA: not available; NF: Neurofilament; NSE: neuron specific enolase; PCNA: proliferating cell nuclear antigen; PR: progesterone receptor; SMA: smooth muscle actin; SSTR2: somatostatin receptor-2; STAT-6: Signal Transducer and Activator of Transcription 6; VIM: vimentin;

Image Differential Diagnosis of ICALM

Because the clinical and imaging characteristics of ICALM are not specific, it is easy to be misdiagnosed. Indeed, some ICALM lesions are accompanied by calcification (3/23, 13.04%), and have the "dural tail sign" (4/54, 7.41%), which makes ICALM more likely to be confused with meningioma. However, meningioma has higher rates of calcification (25%) [11], and the MRI signal of meningioma is mostly similar to the gray matter of the brain. Importantly the MRI T2-weighted signal is lower in meningioma than the signal in ICALM. In addition, the MRI enhancement characteristics of ICALM have "flame" and "salt and pepper" manifestations [12-14]. ICALM demonstrates an early enhanced center in the lesion, and the late enhancement spreads to the periphery of the lesion, suggesting that it may be related to the vascular structure of the lesion. MRI imaging for meningioma usually can be enhanced rapidly after gadolinium injection (except for cases of necrosis and calcification) and does not have the characteristic of progressive enhancement.

Other potentially confounding lesions are schwannomas. Single schwannoma usually occurs along the intracranial nerves, rarely calcification, with about 5% of cases being accompanied by hemorrhage. The schwannoma T1-weighted sequence is hypodense and T2-weighted sequence is hyperdense. Small schwannomas tend to have obvious homogeneous enhancement, while larger diameter schwannomas often have nonhomogeneous signals, often accompanied by necrotic cystic degeneration, in which after the enhancement, the nonhomogeneous enhancement can be observed and the necrotic area of cyst degeneration is not strengthened [7, 15, 16]. For singular or multiple dural metastases, their imaging characteristics may vary greatly due to the different primary lesions, mostly showing

non-specificity and obvious homogeneous enhancement [16, 17]. Accordingly, ICALM can be distinguished from dural metastases by combining the history of the primary diseases and the above characteristics.

Treatment of ICALM and Prognosis

The anatomical structure of ICALM is simple and lacks the main blood supply artery. About 80% (45/54) of the lesions can be completely removed by surgery [9]. Therefore, surgical resection is the preferred treatment regime for ICALM. However, when the neurovascular structure of the location of the lesion is complicated, especially when it occurs in the cavernous sinus, it is very difficult to completely remove ICALM [18]. Digital subtraction angiography (DSA) examination can clearly show the blood supply of ICALM and identify whether it is combined with aneurysm and vascular malformations [19]. DSA-based ICALM preoperative embolization [4, 20, 21] and bipolar cautery [11] have been shown to be effective in reducing intraoperative bleeding and surgical complications. But when ICALM occurs at the base of the skull, it is often difficult to be completely removed due to the abundant blood supply and involvement of important surrounding tissues. Gamma knife radiotherapy can therefore be used to control tumor progression in this type of vascular-rich ICALM [22]. Most patients with ICALM have a good prognosis after surgery. Among the 54 cases studied, only two patients died, one due to surgery while another death was caused by the large tumor that invaded the internal carotid artery [6, 8]. So even though ICALM is benign, it can recur and close follow-up should be given after surgical resection to monitor if new symptoms appear [23].

Conclusions

ICALM is a benign tumor, which is more common in middle-aged men. The CT images of ICALM are mostly slightly high-density, while MRI mainly shows T1-weighted sequence with slightly hypodense, and T2-weighted sequence hyperdense. Enhanced MRI scanning is mostly nonhomogeneous and presents a "flame-like" pattern. Progressive enhancement may be its typical imaging characterization which may help make a clear diagnosis. Fortunately, ICALM can generally be completely removed by surgery. When the blood flow of the lesion is abundant or the anatomical location is complicated, preoperative DSA examination or preoperative embolization is needed and supplementary treatments such as network knife and gamma knife are feasible.

Author Contribution

Aixin Ou and Xiangxuan Zhao designed the study and drafted the manuscript, collected the clinical data and samples, and interpreted the results. All the experiments were completed by Aixin Ou and Xiangxuan Zhao conceived of the study. Xiangxuan Zhao supervised the study, interpreted the results, and revised the manuscript. All authors have approved the final manuscript.

Declaration of Competing Interest

The authors declare that there are no conflicts of interest in this work

Data Availability Statement

The authors confirm that the data supporting the findings of this study are available within the article [and/or] its supplementary materials.

Acknowledgements

This work was partially supported by Basic Scientific Research Project for Natural Sciences in Higher Education Institutions, Liaoning Provincial Department of Education [LJ21251016 2011] to X Zhao.

References

1. McNamara, C., Mankad, K., Thust, S., Dixon, L., Limback-Stanic, C., D'Arco, F., Jacques, T.S., and Lobel, U. (2022). 2021 WHO classification of tumours of the central nervous system: a review for the neuroradiologist. Neuroradiology *64*, 1919-1950.
2. Hachisuga, T., Hashimoto, H., and Enjoji, M. (1984). Angioleiomyoma. A clinicopathologic reappraisal of 562 cases. Cancer *54*, 126-130.
3. Xu, Y., Jing, Y., Ma, S., Ma, F., Wang, Y., Ma, W., and Li, Q. (2010). Primary angioleiomyoma in the sellar region: a case report and literature review. Clin Neuropathol *29*, 21-25.
4. Gasco, J., Franklin, B., Rangel-Castilla, L., Campbell, G.A., Eltorky, M., and Salinas, P. (2009). Infratentorial angioleiomyoma: a new location for a rare neoplastic entity. J Neurosurg *110*, 670-674.

5. Lach, B., Duncan, E., Rippstein, P., and Benoit, B.G. (1994). Primary intracranial pleomorphic angioleiomyoma--a new morphologic variant. An immunohistochemical and electron microscopic study. Cancer *74*, 1915-1920.
6. Sun, L., Zhu, Y., and Wang, H. (2014). Angioleiomyoma, a rare intracranial tumor: 3 case report and a literature review. World J Surg Oncol *12*, 216.
7. Ravikumar, C., Veerendrakumar, M., Hegde, T., Nagaraja, D., Jayakumar, P.N., and Shankar, S.K. (1996). Basal ganglionic angioleiomyoma. Clin Neurol Neurosurg *98*, 253-257.
8. Shinde, S.V., Shah, A.B., Baviskar, R.B., and Deshpande, J.R. (2012). Primary intracranial multicentric angioleiomyomas. Neurol India *60*, 115-117.
9. Colnat-Coulbois, S., Schmitt, E., Klein, O., Weinbreck, N., Auque, J., and Civit, T. (2008). Angioleiomyoma of the cavernous sinus: case report. Neurosurgery *62*, E257-258; discussion E258.
10. Li, C.B., Xie, M.G., Ma, J.P., Wang, L., Hao, S.Y., Zhang, L.W., Jia, W., Jia, G.J., Zhang, J.T., Li, D., et al. (2018). Primary Intracranial Angioleiomyomas as Rare, Nonmalignant, and Distinct Neoplastic Entities: A Series of 8 Cases and a Literature Review. World Neurosurg *113*, 1-13.
11. Chongxiao, L., Wei, S., Yong, L., Qiujuan, Z., Ligui, G., Ren, Z., Jianjun, S., Ruizhi, W., Zhenyu, G., and Xingmiao, L. (2009). Parafalx angioleiomyoma: a case report and review of the literature. BMJ Case Rep *2009*.
12. Altieri, R., Morrone, A., Certo, F., Parisi, G., Buscema, G., Broggi, G., Magro, G., and Barbagallo, G.M. (2019). Tentorial Angioleiomyoma: A Rare Neurosurgical Entity. Case Report and Review of the Literature. World Neurosurg *130*, 506-511.
13. Lee, B., Park, S.J., Moon, J.H., Kim, S.H., Chang, J.H., Kim, S.H., and Kim, E.H. (2019). Angioleiomyoma in the Orbital Apex: A Case Report. Brain Tumor Res Treat *7*, 156-159.
14. Ding, J., Wang, F., Li, Y., and Sun, T. (2020). Rare giant primary intracranial angioleiomyoma in lateral ventricle: a case report and the literature review. Br J Neurosurg *34*, 710-714.
15. Ramesh, P., Annapureddy, S.R., Khan, F., and Sutaria, P.D. (2004). Angioleiomyoma: a clinical, pathological and radiological review. Int J Clin Pract *58*, 587-591.
16. Scherer, K., Johnston, J., and Panda, M. (2009). Dural based mass: malignant or benign. J Radiol Case Rep *3*, 1-12.
17. Lescher, S., Hattingen, E., Franz, K., Mittelbronn, M., and Tews, D.S. (2014). Rare mimicry of meningioma: angioleiomyoma of the falx. J Neurol Surg A Cent Eur Neurosurg *75*, 403-406.
18. Figueiredo, E.G., Gomes, M., Vellutini, E., Rosemberg, S., and Marino, R., Jr. (2005). Angioleiomyoma of the cavernous sinus: case report. Neurosurgery *56*, E411; discussion E411.
19. Xiaofeng, L., Hongzhi, X., and Junrui, C. (2016). Primary Angioleiomyoma in the Cavernous Sinus: A Case Report. World Neurosurg *87*, 661 e617-621.
20. Kohan, D., Downey, L.L., Lim, J., Cohen, N.L., and Elowitz, E. (1997). Uncommon lesions presenting as tumors of the internal auditory canal and cerebellopontine angle. Am J Otol *18*, 386-392.
21. Li, D., Hao, S.Y., Tang, J., Cao, X.Y., Lin, S., Wang, J.M., Wu, Z., Zhang, L.W., and Zhang, J.T. (2014). Primary intracranial angioleiomyomas: diagnosis, treatment, and literature review. Brain Tumor Pathol *31*, 101-107.
22. Stieler, F., Wenz, F., Abo-Madyan, Y., Schweizer, B., Polednik, M., Herskind, C., Giordano, F.A., and Mai, S. (2016). Adaptive fractionated stereotactic Gamma Knife radiotherapy of meningioma using integrated stereotactic cone-beam-CT and adaptive re-planning (a-gkFSRT). Strahlenther Onkol *192*, 815-819.
23. Arat, Y.O., Font, R.L., Chaudhry, I.A., and Boniuk, M. (2005). Leiomyoma of the orbit and periocular region: a clinicopathologic study of four cases. Ophthalmic Plast Reconstr Surg *21*, 16-22.
24. Karagama, Y.G., Bridges, L.R., and van Hille, P.T. (2005). Angioleiomyoma of the internal auditory meatus: a rare occurrence in the internal auditory canal. Ear Nose Throat J *84*, 216, 218.
25. Vijayasaradhi, M., Uppin, S.G., Sreedhar, V., Sundaram, C., and Panigrahi, M.K. (2008). Frontal intradiploic angioleiomyoma. J

Neurosurg Pediatr *2*, 266-268.
26. Pepper, J.P., McKeever, P., Gebarski, S., Spector, M., Thompson, B.G., and Arts, H.A. (2010). Angioleiomyoma of the internal auditory canal: clinical and radiographic features. Otol Neurotol *31*, 1451-1454.
27. Conner, T.M., Waziri, A., and Kleinschmidt-Demasters, B.K. (2012). Angioleiomyomas of the dura: rare entities that lack KRIT1 mutations. Am J Surg Pathol *36*, 526-533.
28. Zhou, Z., Yu, M., Yang, S., Zhou, J., Sun, R., and Yang, G. (2013). Dural angioleiomyoma of the middle cranial fossa: a case report and review of the literature. Brain Tumor Pathol *30*, 117-121.
29. Teranishi, Y., Kohno, M., Sora, S., Sato, H., and Yokoyama, M. (2014). Cavernous sinus angioleiomyoma: case report and review of the literature. J Neurol Surg Rep *75*, e122-128.
30. He, K., Chen, L., Zhu, W., Cheng, H., Wang, Y., and Mao, Y. (2014). Diagnosis and surgical treatment of cavernous sinus angioleiomyoma: a report of four cases. Jpn J Clin Oncol *44*, 1052-1057.
31. Calle, S., Louis, D., Westmark, R., and Westmark, K. (2016). Angioleiomyoma of the falx. J Radiol Case Rep *10*, 8-15.
32. Delgado-Fernandez, J., Penanes, J.R., Torres, C.V., Gordillo-Velez, C.H., Manzanares-Soler, R., and Sola, R.G. (2016). Infratentorial angioleiomyoma: case report and review of the literature. Rev Neurol *62*, 68-74.
33. Selbi, W., Sims-Williams, H., Ince, P., and Carroll, T.A. (2023). Skull base angiomatous leiomyoma: a case report and review of literature. Br J Neurosurg *37*, 668-670.
34. Chen, F., Pan, Y., Teng, Y., Pan, X., and Yu, Y. (2020). Primary Intracranial Angioleiomyoma: A Case Report and Literature Review. World Neurosurg *138*, 145-152.
35. Zhang, S., Wang, Z., Zhang, G., Ji, Y., Wang, Y., and Xiao, S. (2023). Primary angioleiomyoma of right frontal cranial base with intracranial and extracranial communication. Br J Neurosurg *37*, 1010-1015.